OPTIMIZING THE ELECTRICAL CURRENT AND FLUID-FILM THICKNESS TO CONTROL A MAGNETO - RHEOLOGICAL (MR) FLUID BRAKE USING AN ANALYTICAL APPROACH

Salwan Obaid Waheed Khafaji[1][0000-0001-5144-6895], Fawaz F. Al-Bakri[2][0000-0003-1951-5402], Hasan H. Ali[3,][0000-0002-9966-9112]*
[1]Mechanical Power Technical Engineering Department, College of Technical Engineering, Al-Mustaqbal University, 51001, Babylon, Iraq; Al-Mustaqbal Energy Research Center ،Al-Mustaqbal University, Babylon, ,51001, IRAQ.
[2]Department of Biomedical Engineering, College of Engineering, University of Babylon, Babylon, ,51001, IRAQ
[3]Medical Instrumentation Techniques Engineering Department, College of Technical Engineering, Al-Mustaqbal University, Babylon, 51001, IRAQ
* Corresponding author's e-mail: hasan.hamad.ali@uomus.edu.iq (✉)

Abstract - This paper illustrates the first trial of optimizing the magnetorheological fluid brake by analytically controlling the main parameters that conclude its performance. While developing a nonlinear torque model for the brake, a nondimensional analysis is carried out so that the problem is generalized to any brake configuration with similar characteristics while guiding design for comparable strengths of energized and non-energized brake components. The brake speed is using analytical approach using an exponential function for describing shat speed. Lagrange multiplier method is used for seeking the optimal design of the brake parameters as well. This paper shows that the controller guarantees a steady-state solution with zero error in very small time by controlling the fluid thickness and coil current simultaneously. In conclusion, the control method proposed in this paper is shown to increase the operational torque capacity of the brake without increasing the radial dimensions of the brake itself. The Monte-Carlo results showed the validity and robustness of the control method for leading the shaft speed to the desired value in spite of the wide range of dispersion in its initial values.

Keywords: MRF System, Brake System, Monte-Carlo Simulation, Analytical Control, Simulation.

1. Introduction

In rotating mechanical systems, it is standard practice to provide a brake or a rotational damper for speed control. Historically, the brake has adhered to the design of the friction brake, with adverse consequences of excessive wear and premature failure. In this regard, magnetorheological (MR) fluid brakes were introduced for rotational systems, putting an end to material wear and allowing for direct electrical control of the brake. The design of MR fluid brakes is based on the principles of viscous dampers, where fluid shear stress opposes the motion of mechanical parts. In these cases, the strength of the viscous damper is proportional to the fluid viscosity. The novelty of MR fluids consists in the fact that their apparent viscosity can be drastically changed by placing them in an electrically induced magnetic field. By controlling the strength of the magnetics, the viscosity of MR fluid can be easily controlled with very fast response time with a high torque to volume ratio. MR fluid technology holds immense promise in many electrically controlled mechanical systems including brakes and clutches [1,2], vibration control [3], robotic and machinary applications [4], and biomedical applications [5].

An extensive literature on magnetorheological (MR) fluid brakes has been presented by Rossa and colleagues [6]. The authors of the review present the most frequently used models for estimating MR fluid shear-stress, namely the Herschel-Bulkley and Bingham models [7,8]. The authors also address many applications for MR fluid technologies and consider earlier research fields that include optimal design configurations. The optimal design studies seek to minimize system rotating inertia [9], minimize power requirements for operation [10], and maximize torque density with multiple disk employment [11]. Readers are encouraged to refer to these references among others for more examples.

dx.doi.org/10.17683/ijomam/issue24.13

For example, PID control and optimization demonstrates PID and optimized PID (using Fruit Fly, Grey Wolf, GA, and other methods) for real-time MRF brake control, especially for rapid response and reduced overshoot. In general, they are easy in implementation, practical for many scenarios, but limited by system nonlinearities and need for frequent re-tuning [12-16]. Aother researchers discussed how fuzzy and hybrid fuzzy-PID controllers outperform PID in dynamic and uncertain conditions with better robustness, less overshoot, but more design complexity and potential computational burden [17-20]. Moreover, optimization-based and simulation-assisted control explores the application of multi-objective optimization (Genetic Algorithms, Particle Swarm, Nelder–Mead, multidisciplinary design) for integrated mechanical-control design. However, they generally suitable for offline design stages [21-23]. Analytical control strategy is characterized by its accuracy compared to other control methods [24,25]. It was applied to various systems [26] and proved its effectiveness in achieving the desired design specifications in terms of stability and performance.

Literature surveyed and known to the authors demonstrates MR fluid brake control achieved through the current to the electrical coil as a control input. Although this seems the obvious control input, consideration may also be given to control of the brake whereby the input current is altered along with simultaneous changes on the MR fluid thickness. The simultaneous control may be used for a higher torque range without increasing the radial envelope and compensating for saturation limits within electromagnetic fields. This paper sets forth to demonstrate this novel control approach for a single-disk solution and show that good dynamic response can be achieved through the parallel use of two PI controllers.

The main objective of this work is to design a brake system that can properly regulate the shaft speed while considering the constraints set on some system parameters, such as MR fluid thinness and electric current. Controlling a brake system is based on two main concepts; a reference profile is constructed followed by the closed-loop command design for precise tracking of that reference. In this work, reference shaft speed is analytically generated based on the imposed initial and final boundary conditions. The resulting thinness profile of the MR fluid and the electric current profiles are next optimized for the desired shaft speed based on the analytical algorithm, and finally, the proposed system parameters are used to simulate the system. Another great advantage of the analytical control of establishing reference shaft speed on given initial and final boundary conditions for MRF brakes is the customization of speed profile, therefore allowing imposition of exact braking, which is very crucial for safety. By maneuvering MR fluid thickness and electric current profiles, the system properties are brought closer to what is desired as an output, increasing efficiency and response.

Moreover, speed evolution through the three-term exponential function brings dynamism, smoothening out transitions, and handling variable operational conditions. This method also lowers the amount of computation required, thus simplifying simulations and permitting rapid analysis and design modifications important for real-time applications. On top of that, the analytical formulation makes system responses more predictable, thus making the design more reliable. Further, when optimum parameters from the analytical model are used, the accuracy of the simulations increases; this puts a better representation of the actual behavior of the system. In all, it adds unprecedented value to the performance, efficiency, and design procedure of MRF brake systems.

2. MRF Brake Geometry

The schematic representation of a single disc, MR fluid brake is given in Fig. 1. To the left of this figure, there is an unenergized rotating disc connected to a shaft. The angular velocity of the disk is given as ω and the torque generated by the brake is shown by the symbol T. Magneto-rheological (MR) fluid is placed between the moving disk and the non-moving surface, as well as the thickness of the MR fluid as h. In the absence of a magnetic field, MR fluid sustains some shear stress when subjected to shear strain rate proportional with the magnetic shear property that makes non-energized MR fluid behave like a Newtonian fluid with a certain viscosity as far as the flow is concerned. The shear stress in the MR fluid makes its contribution to the brake torque or torsional resistance created by the fluid viscosity at the given angular speed opposed to the MR fluid thickness h.

In the right-hand image of Fig. 1, the same brake geometry is shown, but surrounded by the magnetic field created by passing current through the electric coil wrapped around the brake. The current is shown in Fig. 1 by the symbol entering the coil into the paper from the top and exiting from the paper at the bottom. The unique property of an MR fluid is that when subjected to a magnetic field, the viscosity of the fluid increases. This additional viscosity is increased with increased magnetic-flux density proportional to the current passing through the electric coil. In layman terms, increasing the current in the coil increases the viscosity of the MR fluid and, hence, the resistive torque generated by the brake.

The driving actuator for fluid-thickness settings and coil-current actuation drivers are not presented in Fig. 1; hence, in this research, they will be treated

more or less ideal in nature for the sake of illustration of the control method. The actuator responsible for adjusting fluid thickness will remain relatively small (not requiring any additional radial space); this is justified because low forces will be involved. There are several reasons for the design of a controller modulating both and instead of modulating one alone. Fluid thickness adjustment, by itself, cannot bring a brake fully to rest; hence a control for electric current is required if the intention is to achieve zero velocity. Moreover, the ranges of operation for electric current and fluid thickness are limited, so that once one of the parameters reaches saturation, the other parameter can still control the brake speed. Finally, by adjusting both parameters, the range of braking torque can be extended.

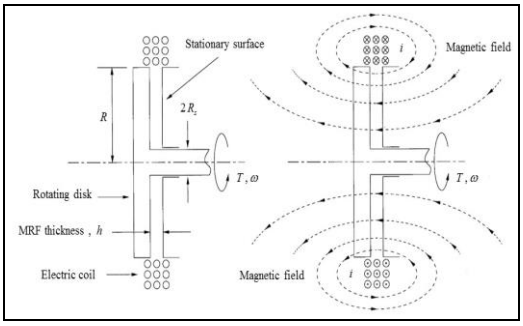

Figure 1: Schematic of the single disk, MR fluid brake [27]

3. System Modelling

Figure 2 shows a schematic of the rotating system that is to be controlled by the MR fluid brake. In this schematic, the left-hand-side represents the MR fluid brake which exerts a control torque *T* on the rotating flywheel. The flywheel is shown to have a mass moment-of-inertia given by *J*. Using a flywheel is an analogy which can be used for different practical application. On the right-hand-side of this schematic, the input torque to the rotating system is given by the load torque T_L. The system rotates about the central axis with an instantaneous angular-velocity ω. Table (1) define the system parameters.

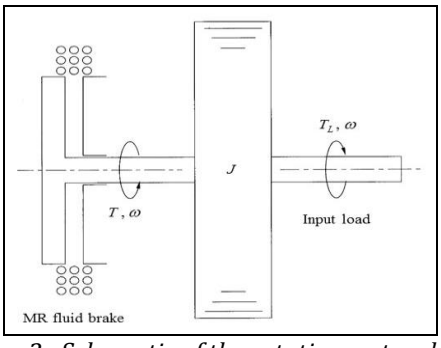

Figure 2: Schematic of the rotating system being controlled by the MR fluid brake [27]

Based on the Newton's second law, equation of motion for the system shown above is given by [24],

$$J\frac{d\omega}{dt} = T_L - T \tag{1}$$

where the symbols t is the time, ω is the instantaneous shaft speed, T is the brake torque, T_L is the applied load torque, and J the mass moment-of-inertia for the flywheel

The mechanical and electrical model of the magnetorheologcial brake will be presented in this section. A front view of the single disk is shown in Fig. 3, where an infinitesimal torque is developed gradually with the speed, on the disk surface by an infinitesimal fluid-shear force *df*. Based on that, torque is expressed as function of the infinitesimal shear force as

$$dT = r\,df \tag{2}$$

Where r the location of the force in the radial direction. Considering that the shear force is $df=2\pi\tau r dr$ and the symbol τ refers to the shear stress of the fluid at the surface of the disk. Then, the total torque developed on the rotated disk by the MR fluid may be represented as [24]

$$T = 2\pi\int_{R_s}^{R}\tau\, r^2\, dr \tag{3}$$

where R is the outer radius of the disk and R_s is the radius of the shaft. As per widely used models in literature regarding shear stress of Bingham fluids, for MR fluids, this shear-stress formulation is given by the Herschel-Bulkley model with (a major provision that when applied to MR fluids) [1,6,7]:

$$\tau = \frac{\mu r\omega}{h} + k\,B^{\alpha} \tag{4}$$

B is the magnetic-flux density generated by the electric coil, h is the instantaneous MR fluid thickness, μ is the absolute viscosity of the non-energized MR fluid, and k and α are material properties for a specific MR fluid. The common value for α=1 [16], and within the boundaries of that linear range of magnetic-flux density as dependent on current, the expression for shear-stress induced by the proper magnetic field would then be given by the following equations.

$$k\,B^{\alpha} = \frac{\tau_B}{i_{max}}\,i \tag{5}$$

where τ_B is the maximum shear yield-stress that may be added to the MR fluid when the maximum allowable current i_{max} is applied to the coil and i is

the electric current. Estimates for τ_B are readily obtained from MR fluid suppliers [13].

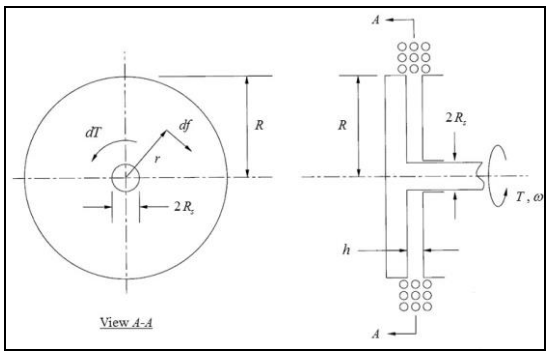

Figure 3: Geometry for the single disk, MR fluid brake [27]

The above equations then can be substituted together to find the total torque as

$$T = \frac{\pi}{2}\frac{\mu\omega}{h}R^4\left[1-\left(\frac{R_s}{R}\right)^4\right] + \frac{2\pi}{3}\tau_B\frac{i}{i_{max}}R^3\left[1-\left(\frac{R_s}{R}\right)^3\right] \quad . \quad (6)$$

The system parameters of the Magneto Rheological Fluid Brake system can be listed in Table (1). These parameters are presented as typical characteristics for a MR fluid brake and their values are physically realistic and may be used to satisfy the design constraint.

Table 1. Magneto Rheological Fluid Brake parameters

Description	**Symbol**	**Value**	**Units**
Nominal MR fluid thickness	h_o	50	μm
Mass moment-of-inertia	J	0.064	kg m^2
Disk radius	R	95	mm
Shaft radius	R_s	20	mm
Nominal brake torque	T_o	53	N m
Characteristic time constant	t_o	0.25	s
MR fluid viscosity	μ	0.1	Pa s
MR fluid maximum shear stress	τ_B	30	kPa
Nominal shaft speed	ω_o	2,000	rpm

Following the previous steps, the total torque, and the other design parameters can be nondimenlized as,

$$h = h_o\,\hat{h} \quad , \quad i = i_{max}\,\hat{i} \quad , \quad R_s = R\,\hat{R}_s \quad ,$$
$$T = T_o\,\hat{T} \quad , \quad T_L = T_o\,\hat{T}_L \quad , \quad t = t_o\,\hat{t} \quad \text{and} \quad \omega = \omega_o\,\hat{\omega} \quad (7)$$

The subindex (o) refers to the parameters at their nominal values. Using the nondimensional representation, Eq. (1) can be given as,

$$\frac{d\hat{\omega}}{d\hat{t}} = \hat{T}_L - \frac{\hat{\omega}}{\hat{h}} - \hat{i} \quad . \quad (8)$$

While the nominal torque and time are given by,

$$T_o = \frac{\pi}{2}\frac{\mu\omega_o}{h_o}R^4\left(1-\hat{R}_s^4\right) \quad \text{and} \quad t_o = \frac{J\,\omega_o}{T_o} \quad . \quad (9)$$

4. Analytical Controller Algorithm

The main objective of this work is to design a brake system that can successfully control the shaft speed while involving the system parameters constraints such as MR fluid thinness and electric current. Commonly, controlling a brake system requires two key concepts; First, a reference profile is shaped, adhered to by the design of a closed-loop command to follow the reference precisely. However, in this study, the reference shaft speed is created analytically based on the initial and final boundary conditions. Then MR fluid thinness and electric current profiles are optimized to capture the desired shaft speed relying on the analytical algorithm. Eventually, the optimal system parameters are used to simulate the system. To do that, the reference shaft speed is parametrized by a three-term exponential function of time as,

$$\omega_{\text{ref}} = \sum_{n=1}^{3} C_n \exp(\kappa n t) \quad (10)$$

The time derivative of Eq. (10) is introduced to compute the shaft acceleration as,

$$\dot{\omega}_{\text{ref}} = \sum_{n=1}^{3} -n\kappa C_n \exp(\kappa n t) \quad (11)$$

As observed from Eqs. (8) and (9), the analytical brake system has three coefficients, so three boundary conditions are required to compute the three coefficients, C_n. Two pairs of shaft speed at the initial and final states and one pair of shaft acceleration at the final state (desired state) are used in this work as,

$$\omega_0 = C_1\exp(\kappa t_0) + C_2\exp(2\kappa t_0) + C_3\exp(3\kappa t_0)$$
$$\omega_d = C_1\exp(\kappa t_f) + C_2\exp(2\kappa t_f) + C_3\exp(3\kappa t_f) \quad (12)$$
$$\dot{\omega}_d = \kappa C_1\exp(\kappa t_f) + (2\kappa)C_2\exp(2\kappa t_f) + 3\kappa C_3\exp(3\kappa t_f)$$

where ω_d is the desired shaft speed.

Substituting the initial and final conditions into Eq. (10), and setting up the equations in matrix form results in,

$$\begin{bmatrix} 1 & 1 & 1 \\ 0.4724 & 0.2231 & 0.1054 \\ -0.071 & -0.067 & -0.0474 \end{bmatrix}\begin{bmatrix} C_1 \\ C_2 \\ C_3 \end{bmatrix} = \begin{bmatrix} \omega_0 \\ 1 \\ 0 \end{bmatrix} \quad (13)$$

So that the numerical values of these coefficients now can be calculated as,

$$C_1 = 0.7955\omega_0 + 4.438$$
$$C_2 = -3.376\omega_0 - 5.344 \quad (14)$$
$$C_3 = 3.58\omega_0 + 0.9$$

Figure (4) shows the exponential coefficients profiles with time. All the function coefficients C1and C_3 increase, while the coefficient C_2 decreases with the initial shaft speed to track the proposed reference and capture the desired shaft speed.

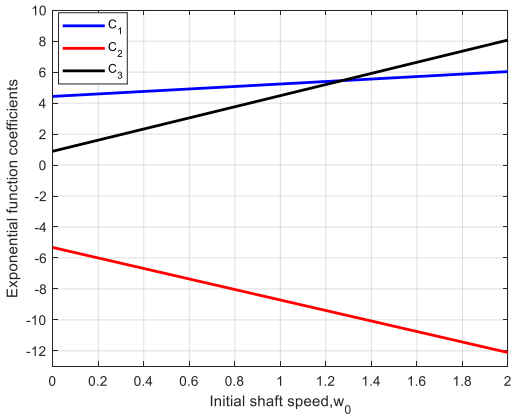

Figure 4: Exponential function coefficients using line equations vs. time.

Substituting Eqs. (12-14) and Eq. (10) to calculate the reference shaft speed as,

$$\omega_{ref} = \begin{pmatrix} \omega_0\begin{pmatrix} 0.7955\exp(-0.15t) - 3.376\exp(-0.3t) \\ +3.58\exp(-0.45t) \end{pmatrix} + \\ \begin{pmatrix} 4.438\exp(-0.15t) - 5.344\exp(-0.3t) \\ +0.9\exp(-0.45t) \end{pmatrix} \end{pmatrix} \quad (15)$$

Equation (15) shows that the reference shaft speed is a function of initial shaft speed and time only. Therefore, it is easily to find the reference shaft speed profile that guides the brake system to capture the desired value when the brake system activates. Figure (5) presents the reference shaft speed profiles for three cases of shaft speed; high, moderate, and low speeds. It can be concluded that the three speed profiles satisfy the initial and final conditions without exhibiting any overshoot behavior and smooth response. Thus, the proposed algorithm can effectively stabilize the brake system for achieving good system characteristics.

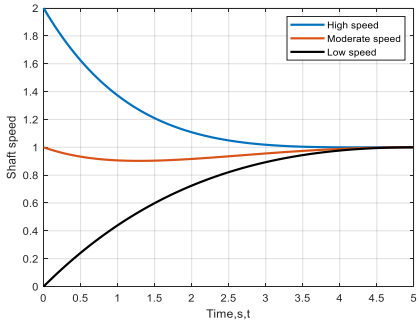

Figure 5: Analytical shaft speed for three initial shaft speeds vs. time.

5. Optimal Brake Parameters

While tracking the references shaft speed, the optimal values of the brake's parameters (MR fluid thickness and electric current) will be taken into the considerations. To solve this optimization problem, Lagrange multipliers method is proposed with the objective function as,

$$f_k(x) = \left|\omega - \omega_{ref}\right|_k \quad \text{where } k = 1,2,3,.....10 \quad (16)$$

where ω and ω_{ref} represent current and reference shaft speeds, respectively.

Recalling, Eq. (8) and solving it with respect to the shaft speed we obtain,

$$\omega = h(t)\left(T_L - \dot{\omega} - i(t)\right) \quad (17)$$

Substituting Eqs. (15) and (17) into Eq. (16) the objective function can be written as,

$$f_k(x) = \left| \left(h(t)\left(T_L - \dot{w} - i(t)\right)\right) - \begin{pmatrix} w_0\begin{pmatrix} 0.7955\,exp(-0.15t) - \\ 3.376\,exp(-0.3t) \\ +3.58\,exp(-0.45t) \end{pmatrix} + \\ \begin{pmatrix} 4.438\,exp(-0.15t) - \\ 5.344\,exp(-0.3t) \\ +0.9\,exp(-0.45t) \end{pmatrix} \end{pmatrix} \right|_k \quad (18)$$

To utilize the optimization method, the Lagrangian function can be obtained,

$$\Im_k\left(x,\lambda_1,\lambda_2\right)=f_k\left(x\right)-\left(\sum\nolimits_{j=1}^{2}\lambda_j g_j\left(x\right)\right)_k \qquad (19)$$

where x is the vector of the optimal parameters (h and i), $f(x)$ and $g_i(x)$ are the objective and constraints functions, respectively, λ_i are Lagrangian multipliers required to satisfy the optimization and k is the time index. In this work, the time vector is divided into ten points along the operation time, so that the optimization process would be applied ten times to get ten optimal values of MRF thickness and current.

To comprehend the proposed optimization methodology, Figs. 6a-6c show the objective function surface used to optimize the nondimensional parameters for high, moderate, and low shaft speeds, respectively. As noticed, the optimization algorithm can successfully compute the optimal fluid thickness and current vectors while preforming completely minimum objective functions for all operational points.

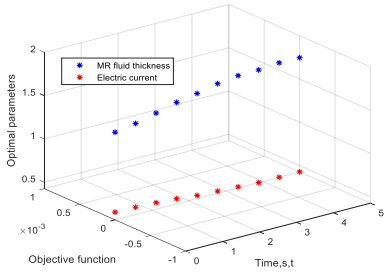

(a)

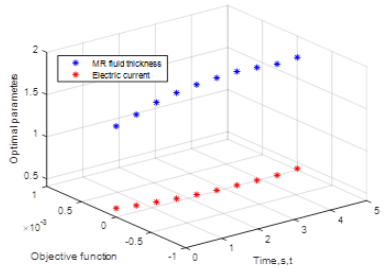

(b)

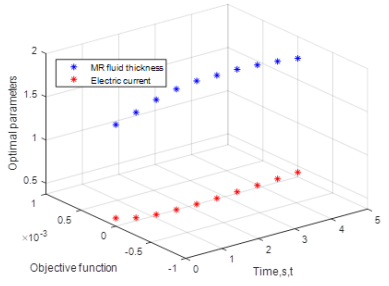

(c)

Figure 6: 3D objective function surface using to optimize the nondimensional parameters for (a) high shaft speed; (b) moderate shaft speed; (c) low shaft speed.

Figures 7a-7c present the analytical responses showing high, moderate, and low shaft speed profiles with time, respectively, using ten optimization points. In each figure, the black lines present shaft speeds, the blue lines display the optimal MR fluid thicknesses, and the red lines display the optimal electrical currents.

Figure 7a shows the initial shaft speed greater than desired speed, wherein initial adjustments must be made by the controller in order to reduce shaft speed. The controller lets first establish a small, saturated MRF fluid thickness to add to the non-energized brake torque, whilst maximizing electric current to apply the maximum energized brake torque. Together, these two mechanisms create major braking force, causing rapid decrease in the shaft speed. As the desired value of the shaft speed is approached, fluid thickness control is relaxed to nominal operating conditions, while the magnetic brake is de-energized gradually. This interactivity ensures that the system can effectively target the shaft speed. As seen, the electric current stabilizes at an optimum value, which is critical for consistent braking performance. The overall response is stable and prompt, with a settling time very close to four time constants. To summarize, the interaction between electric current, fluid film thickness and shaft speed is critical for achieving desired braking performance, thereby underlining the importance of efficient control in MRF-based braking systems.

In Figure 7b, the condition describes a control objective with the same console as before; however, here the initial shaft speed is already close to the desired value. Hence the controller's task becomes one of "keeping" this speed instead of "changing this speed suddenly." The controller maintains a balance in this endeavor by setting a constant value for the optimal MRF fluid thickness while tuning the current to adjust the braking force. In this case, lower electric current has been maintained to produce a controlled but effective braking action on the shaft. The MRF fluid thickness is optimized to stay at a viscosity level where the braking action does not become excessively saturated so as to keep the braking torque constant. This combination allows the shaft speed to fluctuate around the desired value, which over time remains more or less constant regarding fluid thickness and electric current, thus demonstrating a well-tuned control system acting alongside the dynamics of the MRF brake. The small fluctuations of the shaft speed signify the operating stability of the system.

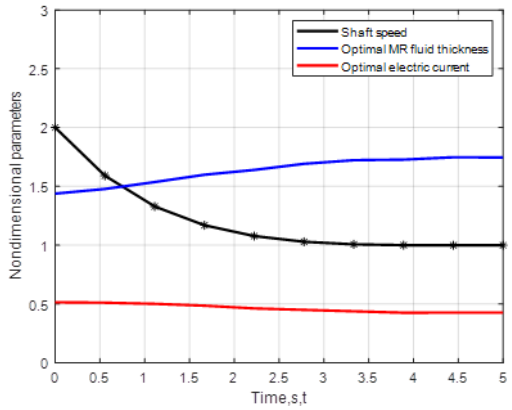

(a)

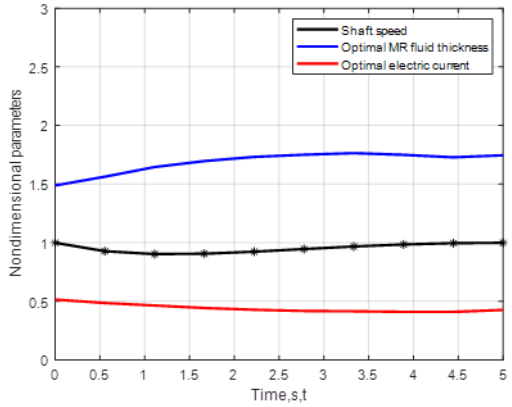

(b)

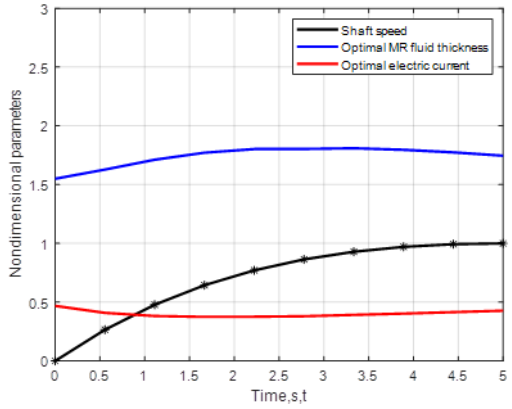

(c)

Figure 7: Analytical response illustrating high speed control for using ten optimization points for (a) high shaft speed; (b) moderate shaft speed; (c) low shaft speed

Finally, in Fig 7c is the case where the control objective is to let the shaft speed increase to the target after the initial shaft speed is much lower than the desired value. Increasing the MRF fluid thickness quickly to the optimal level was then made, minimizing the nonenergized brake torque, thus permitting more aggressive acceleration. Such paradigms to increase fluid thickness ensure that the braking force is well adjusted to aid the desired acceleration of the shaft. Meanwhile, the current was lowered to reduce the energized braking force, which in turn helped to accelerate the shaft speed to the desired one. The graph indicates that the shaft speed rises steadily, approaching the desired speed as the control system balances the competing requirements of torque and fluid dynamics.

The fluid-thickness control for smooth operation is gradually reduced to nominal levels as the shaft speed tends toward the target and to mitigate sudden changes. These independent changes lead to a stable response with a four-time constant settling time. Such an increase may incur some overshoot, depicting the natural tendencies of the system to accelerate and stabilize. Thus, the strategy used must rapidly adjust to changing conditions in performance.

In this regard, the interplay between electric current, MRF fluid thickness, and shaft speed illustrates the efficiency of the MRF brake control mechanisms to deliver acceleration while maintaining stable operation on its way to the desired shaft speed. The proposed algorithm requires two basics: shaping a reference shaft speed profile relying in the initial shaft speed. Then computing the MR fluid thickness and electrical current profiles required to track the reference shaft speed and achieve the desired shaft speed.

6. Numerical Simulation

Most magnetorheological fluid systems aim to control the shaft speed while maintaining the electrical current and fluid thickness from exceeding the maximum limits. This objective can usually be done by generating a reference path first, then adopting control methods to pursue it. Our algorithm is totally dissimilar other previous control methods. The proposed approach can guide the system to capture the desired shaft speed while optimizing the electrical current and fluid thickness profiles instantaneously, to perform the minimum objective functions for all operational points. In conclusion, Eq. (18) is the objective function that needs to be minimized in order to track the reference shaft speed, Eq. (15), while optimizing the electrical current and fluid thickness parameters presented in Fig. 6.

Figures 8a-3c, show the analytical and simulated shaft speeds for high, moderate, and low initial shaft speeds, respectively. Figure 8a shows that both of the consistent system's responses decay exponentially with no chance of overshot to reach the desired shaft speed in roughly 3.5 sec. While below the moderate initial shaft speed, as indicated in Fig 8b, the shaft speed profiles first drop and then ascent to attain the target state in an estimated time of 5 sec. In reality, this behavior occurs due to the proximity between the initial and desired shaft speeds, thus the system needs to undershoot its

shaft speed reaching the steady state condition. Eventually, Fig. 8c presents a gradually ascent throughout the simulation taking approximately 5sec to stabilize the system. With the application of the optimal electrical current and fluid thickness profiles, Fig. 8 shows that the MR fluid system is remarkably qualified to track the reference shaft speeds without requiring any feedback control.

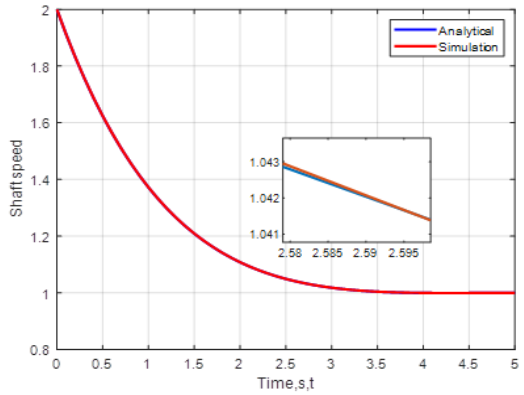

(a)

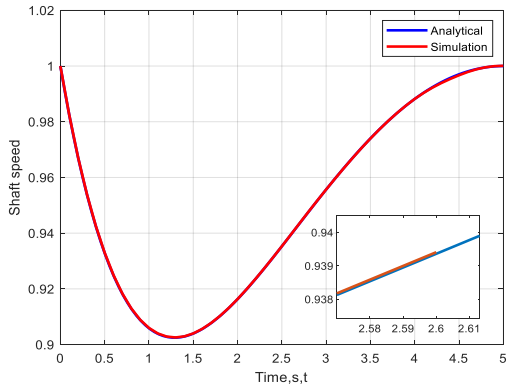

(b)

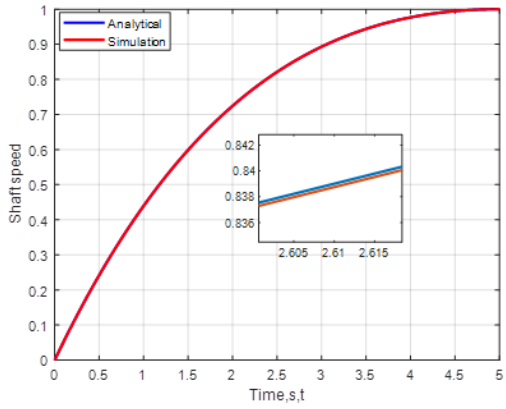

(c)

Figure 8: Analytical and simulated shaft speed for different initial shaft speed; (a) high initial shaft speed; (b) moderate initial shaft speed; (c) low initial shaft speed.

It seems unlikely that the magnetorheological fluid brake system work under nominal initial shaft speeds since the system may be initiated with different initial speeds. Therefore, it is significantly important to include off-nominal initial shaft speed to test the performance of the system which will be addressed in the next section.

7. Monte-Carlo Simulation

Monte Carlo simulation is a standard technique for simulating dispersions the in system parameters. It can be used for ensuring robust, accurate, and effective designs [28]. Monte Carlo tests show the performance and reliability of the control of the MRF brake system under various conditions. The repeated stabilization of the shaft speed over many runs indicates that the control strategy is capable of cancelling disturbances sufficiently so as to allow the system to respond adaptively. The control strategy seems to actively intervene to set the desired shaft speed, either through electrical current or fluid thickness adjustments. Thus, the interaction between electric current with MRF fluid thickness and shaft speed shows the control strategies ability in exerting influence on the MRF brake system. The Monte Carlo results also give an indication of reliability and robustness in the system, further supporting its enhanced ability to sustain performance under various operating conditions.

In addition, on observation, the ranges of electric current and thickness of MRF fluid do possess relatively small ranges compared with that of shaft speed at the beginning (time=0). And this is quite interesting for various reasons: first, the small range in electric current and fluid thickness reveals that the system is actually able to control well through a wide initial range of shaft speeds, which means that even minor variations in these parameters lead to a significant change in performance, enabling the system to adapt well to changes in condition. Secondly, although there is a high dispersion in the initial shaft speed, the control can still be maintained, which shows robustness in the control strategy. This means that the system can tolerate very wide ranges in speed but needs very small changes in the control parameters (current and fluid thickness). Thirdly, this makes practical requirement easier for operation of the system in the field. The engineers would get the level of performance they desired without necessity to carry out extensive tuning of the control settings. It simplifies demands of operation in the field while reducing system tuning complexity.

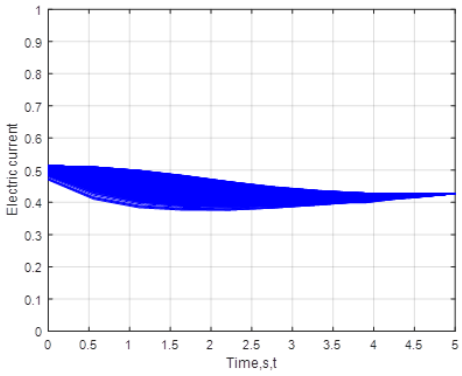

(a)

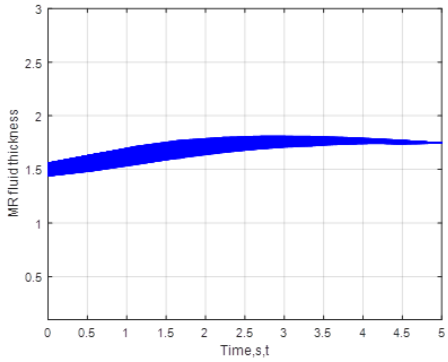

(b)

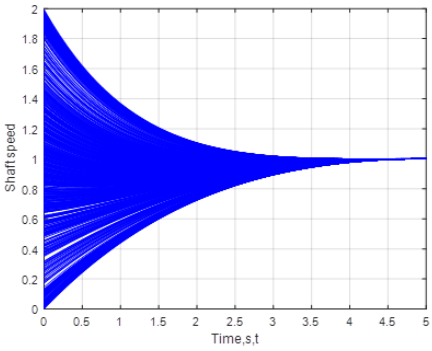

(c)

Figure 9: Hysterical results for 500 initial shaft speed; (a) electric current vs. time ;(b) MR fluid thickness vs. time; (c) shaft speed vs. time.

8. Conclusions

The analysis, results, and discussion in the paper offer support for the conclusions listed below.

1. An MR fluid brake is capable of generating torque from two sources: (i) a non-energized source (caused by the action of viscosity due to Newtonian viscosity, angular velocity, and thickness of MR fluid), and (ii) an energized source brought about by the less viscous MR fluid under presence of a magnetic field.

2. The result from the simultaneous control of the thickness of the MR fluid and the electric current is a very wide range of brake torque without increase of the radial envelop for the brake, and saturation conditions in one controller are compensated for by the other one. Primarily high angular velocities of the brake are controlled with increasing thickness of the MR fluid while low angular velocities are controlled mainly by switching the increased intensity of the electric current.

3. The equation governing angular velocity of brake could be such that quite elegant forms are presented by nondimensional analysis. The overall phenomena of this problem are captured by three things: i) the nondimensional loading-torque applied, ii) the nondimensional MR fluid thickness, and iii) the nondimensional electric current. Any change in one of these things will affect the dynamic and steady-state response of the brake.

4. The interplay between electric current, MRF fluid thickness, and shaft speed illustrates the efficiency of the MRF brake control mechanisms to deliver acceleration while maintaining stable operation on its way to the desired shaft speed.

5. The proposed analytical control strategy has been well able to steer the system to a stable desired state with smooth response even in the presence of uncertainties and dissatisfactions in initial conditions.

6. Using the analytical controller make the practical requirement easier for operation of the system in the field. The engineers would get the level of performance they desired without necessity to carry out extensive tuning of the control settings. It simplifies demands of operation in the field while reducing system tuning complexity.

References

[1] Li, W.H., and H. Du. 2003. Design and experimental evaluation of magnetorheological brake. The International Journal of Advanced Manufacturing Technology. 21:508-515, pp. 508-15.

[2] Haung, J., J.Q. Zhang, Y. Yang, Y.Q. Wei. 2002. Analysis and design of a cylindrical magneto-rheological fluid brake. Journal of Materials processing Technology. 129:559-62.

[3] Duan, Y.F., Y.Q. Ni, and J.M. Ko. 2006. Cable vibration control using magnetorheological dampers. Journal of Intelligent Material Systems and Structures. Vol 17, No. 4, pp. 321-25.

[4] Kikuchi, T., K. Oda, and J. Furusho. 2010. Leg-robot for demonstration of spastic movements of brain-injured patients with compact magnetorheological fluid clutch. Advanced Robotics. Vol. 24, No. 5/6, pp. 671-86.

[5] Chen, J.Z., and W.H. Liao. 2010. Design, testing, and control of magnetorheological actuator for assistive knee braces. Smart Materials and Structures. Vol. 129, No. 3, p. 035029.

[6] Rossa, C., A. Jaegy, J. Lozanda, and A. Micaelli. 2014. Design considerations for magnetorheological brakes. IEEE/ASME Transactions on Mechatronics. Vol. 19, No. 5, pp. 1669-80.

[7] Lee, D., and N.M. Wereley. 2000. Analysis of electro- and magneto-rheological flow mode dampers using Herschel-Bulkley model. Proceedings of SPIE. Vol. 3989, No. 1, pp. 244-55.

[8] Lindler, J., and N.M. Wereley. 2003. Quasi-steady Bingham plastic analysis of an electrorheological flow mode bypass damper with piston bleed. Smart Materials and Structures. Vol 12, No. 3, pp. 305-17.

[9] Kikuchi, T., and K. Kobayashi. 2011. Development of cylindrical magnetorheological fluid brake for virtual cycling system. IEEE International Conference on Robotics and Biomimetics. Pp. 2386-92.

[10] Shiao, Y.J., and C.Y. Chang. 2011. Design of an innovative high-torque brake. Advanced Materials Research. Vol. 339, pp. 84-87.

[11] Nikitczuk, J., B. Weinberg, and C. Mavroidis. 2007. Control of electro-rheological fluid based resistive torque elements for using in active rehabilitation devices. Smart Materials and Structures. Vol. 16, No. 2, pp. 418-28.

[12] Zainordin et al., "The Magnetorheological Fluid: Testing on Automotive Braking System," Int. J. Automotive Mechanical Engineering, 2021.

[13] Dai, L., Lu, H., Hua, D., Liu, X., Wang, L. and Li, Q., 2022. Research on control strategy of a magnetorheological fluid brake based on an enhanced gray wolf optimization algorithm. *Applied sciences*, *12*(24), p.12617.

[14] Liu, X., Shi, Y. and Xu, J., 2017. Parameters tuning approach for proportion integration differentiation controller of magnetorheological fluids brake based on improved fruit fly optimization algorithm. Symmetry, 9(7), p.109.

[15] Bazargan-Lari, Y., 2019. Design and shape optimization of MR brakes using Nelder–Mead optimization algorithm. Mechanics & Industry, 20(6), p.602.

[16] Hoang, Q.T., Trinh, M.H. and Nguyen, T.T., 2024. Simulation of Auxiliary Magnetorheological Brake on Vehicles. Journal of Transportation Technologies, 15(1), pp.122-134.

[17] Hua, D., Liu, X., Gupta, M.K., Fracz, P. and Li, Z., 2021. A new combined braking approach of magnetorheological fluids brake based on fuzzy controller and improved PID controller. Proceedings of the Institution of Mechanical Engineers, Part C: Journal of Mechanical Engineering Science, 235(23), pp.6644-6658.

[18] Adiputra, D., Ubaidillah, U., Mazlan, S.A., Zamzuri, H. and Rahman, M.A.A., 2016. Fuzzy logic control for ankle foot orthoses equipped with magnetorheological brake. Jurnal Teknologi (Sciences & Engineering), 78(11).

[19] Rashid, M.M., Hussain, M.A., Rahim, N.A. and Momoh, J.S., 2009. Development of fuzzy logic controller for magnetorheological rotary brake system. International Journal of Mechanical and Materials Engineering, 4(3), pp.232-238.

[20] Wang, Z. and Choi, S.B., 2021. A fuzzy sliding mode control of anti-lock system featured by magnetorheological brakes: Performance evaluation via the hardware-in-the-loop simulation. Journal of Intelligent Material Systems and Structures, 32(14), pp.1580-1590. [21] Design and shape optimization of MR brakes using Nelder–Mead optimization algorithm," Mechanics & Industry.

[21] Topcu, O., Taşcıoğlu, Y. and Konukseven, E.I., 2018. Design and multi-physics optimization of rotary MRF brakes. Results in physics, 8, pp.805-818.

[22] Turabimana, P. and Sohn, J.W., 2023, August. Optimal design and control performance evaluation of a magnetorheological fluid brake featuring a T-shape grooved disc. In Actuators (Vol. 12, No. 8, p. 315). MDPI.

[23] Al-Bakri, F.F., Ali, H.H. and Khafaji, S.O.W., 2024. Adaptive control of a submarine for various diving depths using an exponential function. *Jurnal Teknologi (Sciences & Engineering)*, *86*(4), pp.79-86.

[24] Ali, H.H., Khafaji, S.O.W., Al-Bakr, F.F. and Aubad, M.J., 2024. Design of a Motion Control for a Hydraulic Rotary Actuator Using a Variable Displacement Pump. International Journal of Mechatronics and Applied Mechanics, (18), pp.60-66.

[25] Ali, H.H., Al-Bakri, F.F. and Khafaji, S.O.W., 2023. Analytical Position Control System of a Linear Hydraulic Actuator Used in Aircraft Applications. International Journal of Mechatronics and Applied Mechanics, (13), pp.209-218. https://doi.org/10.17683/ijomam/issue13.25.

[26] Khafaji, S.O.W., Ali, H.H., Al-Bakri, F.F., Manring, N.D. (2025). Controlling a Magnetorheological (MR) Fluid Brake by Simultaneously Adjusting the Electrical Current and the Fluid-Film Thickness. In: Cioboată, D.D., Machado, J. (eds) International Conference on Reliable Systems Engineering (ICoRSE) - 2025. ICoRSE 2025. Lecture Notes in Networks and Systems, vol 1592. Springer, Cham. https://doi.org/10.1007/978-3-032-02508-1_12.

[27] Wakefield, A.; Miller, S. Improving System Models by Using Monte Carlo Techniques on Plant Models. In Proceedings of the AIAA Modelling and Simulation Technologies Conference and Exhibit. American Institute of Aeronautics and Astronautics, Honolulu, HI, USA, 18-21 August 2008.